Journal of Applied Physics

RESEARCH ARTICLE | MAY 20 2021

Quantum flexoelectric nanobending

Special Collection: Trends in Flexoelectricity

Fredy Zypman

J. Appl. Phys. 129, 194305 (2021)
https://doi.org/10.1063/5.0048724
CHORUS

Journal of Applied Physics ARTICLE scitation.org/journal/jap

Quantum flexoelectric nanobending

Cite as: J. Appl. Phys. **129**, 194305 (2021); doi: 10.1063/5.0048724
Submitted: 25 February 2021 · Accepted: 6 May 2021 ·
Published Online: 20 May 2021

Fredy Zypman[a)]

AFFILIATIONS

Department of Engineering Physics, Yeshiva University, 2495 Amsterdam Avenue, Manhattan, New York 10033, USA

Note: This paper is part of the Special Topic on Trends in Flexoelectricity.
[a)]**Author to whom correspondence should be addressed:** zypman@yu.edu

ABSTRACT

The aim of this article is twofold. First, to develop a clear quantum theoretical playground where questions about the connection between strain fields and electric fields could be unambiguously explored. Second, as an application, to derive a criterion that establishes the length scale below which bent molecules, in particular, carbon nanotubes, display flexoelectricity. To this end, we consider a model molecule that displays the basic elements necessary to support flexoelectricity. Due to its simplicity, a full quantum mechanical solution is possible, providing analytical expressions for the energy bands and for the electronic states and their corresponding strain gradient-induced charge density. This charge density is in turn used to evaluate the appearance of electric fields. Finally, we investigate the consequences of applying our model to real organic ring systems, in particular, answering the question of whether flexoelectricity found in the theory should be present in experiments.

I. INTRODUCTION

While flexoelectricity was first predicted theoretically by Kogan over half a century ago,[1] it has not been until the last few years that a revived interest in the subject has arisen, due mainly to the technological ability and to the desire to build sensors and actuators at the sub-micrometer scale, where flexoelectricity is expected to play a key role, but also for its intrinsic scientific value. Moreover, 50 years elapsed since the description of the inverse flexoelectric effect[2] and that of connections of the converse effect with piezoelectricity.[3]

Although the high activity on flexoelectricity has clearly established its ubiquity at the sub-micrometer scale,[4–10] and substantial conceptual progress has been made, fundamental questions still mar its interpretation, in particular, the comparison between theory and experimental results. Indeed, flexoelectricity is inextricably convolved with piezoelectric and semiconducting properties. For example, piezoelectric coefficients go hand-in-hand with permittivity,[11] and surface piezoelectric effects[12] or asymmetric piezoelectricity[13] may not be distinguishable from flexoelectricity.

Here, we study theoretically, from a quantum mechanics perspective, the appearance of flexoelectricity on bent molecules. The molecular system is chosen so that charge redistributions by bending are purely flexoelectric. Also, the experimental measurement of charge at the nanoscale is coming of age; assessing quantitative charge values is now possible.[14,15] Thus, this theoretical model becomes ideal for a direct check of foundational flexoelectricity.

While our goal here is to present a system that can be solved completely analytically to gain insight into its physics, the formalism is readily generalizable to more complex molecules in case, to compare with specific experiments, more accurate answers were required.

The paper is organized as follows. In Sec. II, we present the Hamiltonian for the bent molecular chain and find the energy bands and states. In Sec. III, we obtain the electron probability density of the system by considering the filling of all states up to the Fermi level. In Sec. IV, we use the probability density to calculate the charge separation of the system and the concomitant-induced electric quadrupole. We apply the results to organic molecules that have been recently synthesized. In Sec. V, conclusions, we put the main results of the paper in context, mention ways in which the framework could be used to understand other systems and suggest experiments that may measure this flexoelectric charge separation.

II. ELECTRONIC STATES

Consider two identical parallel chains of M atoms each, adjacent atoms being separated a distance δ, with $(M-1)\delta = L$, the length of the system.

Figure 1(a) shows a diagram of the unbent system, and, considering nearest neighbor interactions, the tight binding Hamiltonian[16] is

$$H_{\text{straight}} = \sum_{m_o=1}^{M} \alpha|m_o\rangle\langle m_o| + \sum_{m_i=1}^{M} \alpha|m_i\rangle\langle m_i| + \sum_{m_i=1}^{M-1} \beta(|m_i+1\rangle\langle m_i| + |m_i\rangle\langle m_i+1|) + \sum_{m_o=1}^{M-1} \beta(|m_o+1\rangle\langle m_o| + |m_o\rangle\langle m_o+1|) + \sum_{m_o=1}^{M} \beta|m_i\rangle\langle m_o|\,\delta_{m_i m_o}, \quad (1)$$

where α is the onsite parameter, β is the hopping parameter,[17] and $\delta_{m_i m_o}$ is the Kronecker delta: $\delta_{m_i m_o} = 1$ if $m_i = m_o$ and $\delta_{m_i m_o} = 0$ if $m_i \neq m_o$. The state $|m_o\rangle$ represents the atomic orbital at site m_o of the outer (orange) ring, and the state $|m_i\rangle$ represents the atomic orbital at site m_i of the inner (indigo) ring, with $1 \leq m_{oi} \leq M$. A simpler way to track the site location can be achieved by introducing the spinors

$$|m_o\rangle = \begin{pmatrix} |m_o\rangle \\ 0 \end{pmatrix}, \quad (2a)$$

$$|m_i\rangle = \begin{pmatrix} 0 \\ |m_i\rangle \end{pmatrix}, \quad (2b)$$

so that, for example, $\begin{pmatrix} |5\rangle \\ 0 \end{pmatrix}$ represents the atomic orbital at site 5 of the orange ring.

Next, consider bending the straight molecule of Fig. 1(a) into a circle [Fig. 1(b)] of radius R such that $2\pi R = (M-1)\delta$. On bending, the outer (orange) atoms will be farther apart than δ, and the inner (indigo) atoms will be closer than δ. Specifically, those separations are $\delta\left(1 \pm \frac{\delta}{2R}\right) = \delta\left(1 \pm \frac{\pi}{M-1}\right)$. This has the effect of changing the hopping parameters of the tight binding Hamiltonian. Indeed, since the hoping parameter diminishes exponentially with atomic separation,[18] we have

$$\text{hoping parameter} = \text{constant}\exp\left[-\kappa\delta\left(1 \pm \frac{\delta}{2R}\right)\right] = \text{constant}\exp(-\kappa\delta)\exp\left(\mp\frac{\kappa\delta^2}{2R}\right). \quad (3)$$

We notice that the combination constant $\exp(-\kappa\delta)$ is the native β, as in the straight chain. Then, we have that

$$\text{hoping parameter} = \beta\exp(\pm\Delta), \quad (4)$$

with the definition of the dimensionless constant $\Delta = \frac{\kappa\delta^2}{2R} = \frac{\pi\kappa\delta}{M-1}$.

Thus, the Hamiltonian for the straight system [Eq. (1)] is modified for the bent molecule as follows:

$$H = \sum_{m_o=1}^{M} \alpha|m_o\rangle\langle m_o| + \sum_{m_i=1}^{M} \alpha|m_i\rangle\langle m_i| + \sum_{m_i=1}^{M} \beta e^{-\Delta}(|m_i+1\rangle\langle m_i| + |m_i\rangle\langle m_i+1|) + \sum_{m_o=1}^{M} \beta e^{+\Delta}(|m_o+1\rangle\langle m_o| + |m_o\rangle\langle m_o+1|) + \sum_{m_o=1}^{M} \beta|m_i\rangle\langle m_o|\,\delta_{m_i m_o}, \quad (5)$$

where the hopping parameter has been upgraded and all the sums run to M, with the understanding that the index $M+1$ corresponds to index 1, corresponding to the circular molecule. In addition, the hoping parameter in the last term is the same as in Eq. (1), because the separation between nearest neighbors from the two chains remains unchanged.

Using the notation from Eq. (2), we write the eigenvectors of H [Eq. (5)] as

$$|\varphi_n\rangle = \sum_{m=1}^{M} \begin{pmatrix} T_{om}|m\rangle \\ T_{im}|m\rangle \end{pmatrix}, \quad (6)$$

where T_{om} is the amplitude of the eigenstate n at the outer site located at m and the same for index i.

Due to the $C_{2\pi}$ rotational symmetry, the coefficients are of the form

$$T_{om} = T_o\, e^{im\theta}, \quad (7a)$$

$$T_{im} = T_i\, e^{im\theta}, \quad (7b)$$

where

$$\theta = \frac{2\,\pi\,n}{M}, \quad (8)$$

with n an integer between 0 and $M-1$.

The coefficients T_o and T_i are obtained by considering Schrödinger Equation $H|\phi_n\rangle = E|\phi_n\rangle$ with the Hamiltonian in

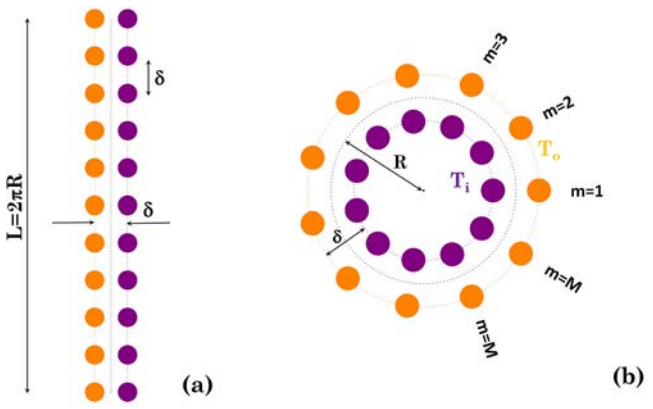

FIG. 1. A straight double chain of atoms (a) of length L and width δ is bent into a circle (b) or radius R. Although all atoms are identical, here we explicitly differentiate the outer (orange) from the inner (indigo).

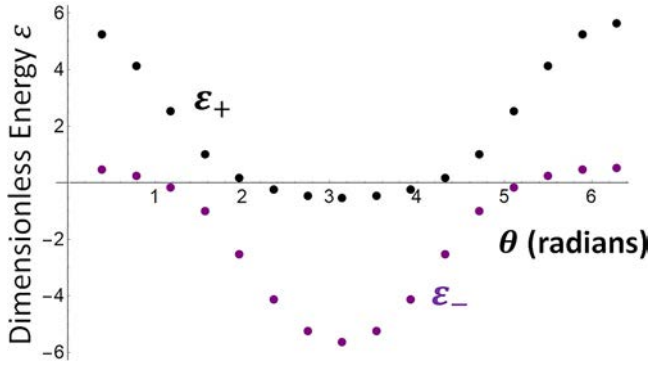

FIG. 2. The two energy bands of Eq. (11) for $\Delta = 1$ and $M = 16$. In this case, we see visually that the top of the bottom 16 energy states (HOMO) is slightly below the $\varepsilon = 0$ line.

Eq. (5) and using Eqs. (7) and (6). Upon performing those substitutions,

$$\begin{pmatrix} \alpha + 2\beta e^{-\Delta}\cos\theta & \beta \\ \beta & \alpha + 2\beta e^{+\Delta}\cos\theta \end{pmatrix}\begin{pmatrix} T_o \\ T_i \end{pmatrix} = E\begin{pmatrix} T_o \\ T_i \end{pmatrix}. \quad (9)$$

It is convenient to introduce the dimensionless energy $\varepsilon = \frac{E-\alpha}{\beta}$, with which Eq. (9) becomes

$$\begin{pmatrix} 2e^{-\Delta}\cos\theta - \varepsilon & 1 \\ 1 & 2e^{+\Delta}\cos\theta - \varepsilon \end{pmatrix}\begin{pmatrix} T_o \\ T_i \end{pmatrix} = 0. \quad (10)$$

The two solutions for ε correspond to two energy bands

$$\varepsilon_\pm = 2\cos\theta\cosh\Delta \pm \sqrt{1 + 4\cos^2\theta\sinh^2\Delta}, \quad (11)$$

with θ given in Eq. (8). Figure 2 shows a typical energy band structure for the system.

From Eq. (11), for each of the M values of θ, there are two energy states, so that the system has 2M states in total, and at low temperatures, half of them are occupied with two electrons each, up to the topmost energy, the Fermi energy. For large M, the Fermi energy for this system is zero, but for $M<10$, there are slight deviations that affect the electric properties.

The coefficients T_o and T_i for each energy are readily computed,

$$T_o^\pm = \frac{1}{\sqrt{1 + (\varepsilon_\pm - 2\cos\theta\, e^{-\Delta})^2}}, \quad (12a)$$

$$T_i^\pm = \frac{\varepsilon_\pm - 2\cos\theta\, e^{-\Delta}}{\sqrt{1 + (\varepsilon_\pm - 2\cos\theta\, e^{-\Delta})^2}}, \quad (12b)$$

where we have chosen normalization $|T_o^\pm|^2 + |T_i^\pm|^2 = 1$.

Finally, the eigenstates (6) take the explicit form

$$|\varphi_\theta^\pm\rangle = \frac{1}{M}\begin{pmatrix} T_o^\pm \\ T_i^\pm \end{pmatrix}\sum_{m=1}^{M} e^{im\theta}|m\rangle. \quad (13)$$

III. ELECTRON PROBABILITY DENSITY

From Eq. (13), the probability to find an electron in state θ in the outer ring (regardless of location) is $\frac{1}{M}(|T_o^+|^2 + |T_o^-|^2)$. Then, the probability of finding an electron in the outer ring (regardless of state) should consider all states with energies below the Fermi energy,

$$P_o = \frac{1}{M}\left(\sum_{\theta_+}|T_o^+|^2 + \sum_{\theta_-}|T_o^-|^2\right), \quad (14)$$

where θ_+ represents the states of the upper band (ε_+) with energies $\varepsilon(\theta_+) \le \varepsilon_F$ and θ_- labels the states of the lower band (ε_-) with $\varepsilon(\theta_-) \le \varepsilon_F$.

Similarly, the probability of finding an electron in the inner ring (regardless of state) considers all states with energies below the Fermi energy,

$$P_i = \frac{1}{M}\left(\sum_{\theta_+}|T_i^+|^2 + \sum_{\theta_-}|T_i^-|^2\right) = 1 - P_o. \quad (15)$$

Equations (14) and (15) serve as the basis to understand the charge unbalance upon bending. The probabilities, through the T coefficients, depend on M and thus on the curvature.

The expression for P_o in Eq. (14) can be made more explicit by noticing that, from Eqs. (11) and (12),

$$|T_o^\pm|^2 = \frac{1}{2} \pm \frac{\cos[\theta]\sinh[\Delta]}{\sqrt{1 + 4\cos[\theta]^2\sinh[\Delta]^2}}. \quad (16)$$

Thus,

$$P_o = \frac{1}{M}\left[\sum_{\theta_+}\left(\frac{1}{2} - \frac{\cos[\theta]\,\sinh[\Delta]}{\sqrt{1+4\,\cos[\theta]^2\,\sinh[\Delta]^2}}\right) + \sum_{\theta_-}\left(\frac{1}{2} + \frac{\cos[\theta]\,\sinh[\Delta]}{\sqrt{1+4\,\cos[\theta]^2\,\sinh[\Delta]^2}}\right)\right]. \tag{17}$$

Since there are M occupied states below the Fermi level, $\sum_{\theta_+} 1 + \sum_{\theta_-} 1 = M$; therefore,

$$P_o = 1 + \frac{1}{M}\left[\sum_{\theta_-}\left(\frac{\cos[\theta_-]\,\sinh[\Delta]}{\sqrt{1+4\,\cos[\theta_-]^2\sinh[\Delta]^2}}\right) - \sum_{\theta_+}\left(\frac{\cos[\theta_+]\,\sinh[\Delta]}{\sqrt{1+4\,\cos[\theta_+]^2\,\sinh[\Delta]^2}}\right)\right]. \tag{18}$$

IV. CHARGE SEPARATION AND INDUCED QUADRUPOLE

Each site, m, of the outer ring contributes a fixed positive nuclear charge e and a negative electronic charge $-e\,P_o$. Thus, each site of the outer ring has a net charge $q_o = (1 - P_o)e$, and similarly, each site of the inner ring has a net charge $q_i = -(1 - P_o)e$. Using Eq. (18),

$$q_o = \frac{e}{M}\left[\sum_{\theta_+}\left(\frac{\cos[\theta_+]\sinh[\Delta]}{\sqrt{1+4\,\cos[\theta_+]^2\sinh[\Delta]^2}}\right) - \sum_{\theta_-}\left(\frac{\cos[\theta_-]\sinh[\Delta]}{\sqrt{1+4\,\cos[\theta_-]^2\sinh[\Delta]^2}}\right)\right], \tag{19a}$$

$$q_i = -q_o. \tag{19b}$$

This charge separation produces a quadrupole moment $\mathcal{Q}$, and we proceed to calculate it. Starting from its definition,[19]

$$\mathcal{Q} = \sum_{k=\text{atom position}} q_k(3\,\vec{r}_k\vec{r}_k - r_k^2\,\mathbb{I}), \tag{20}$$

where $\mathbb{I}$ is the two-dimensional identity matrix, $\vec{r}_k$ is the position of atom k, and $\vec{r}_k\vec{r}_k$ is the dyadic[20] of $\vec{r}_k$ with itself.

Accounting explicitly for the M sites in each ring and writing the matrices of Eq. (20) explicitly,

$$\mathcal{Q} = q_o\sum_{m=1}^{M}\left[3\begin{pmatrix} x_{om}^2 & x_{om}y_{om} \\ x_{om}y_{om} & y_{om}^2\end{pmatrix} - \begin{pmatrix} x_{om}^2+y_{om}^2 & 0 \\ 0 & x_{om}^2+y_{om}^2\end{pmatrix}\right] - q_o\sum_{m=1}^{M}\left[3\begin{pmatrix} x_{im}^2 & x_{im}y_{om} \\ x_{im}y_{im} & y_{im}^2\end{pmatrix} - \begin{pmatrix} x_{im}^2+y_{im}^2 & 0 \\ 0 & x_{im}^2+y_{im}^2\end{pmatrix}\right], \tag{21}$$

with

$$\begin{cases} x_{om} = \left(R + \frac{\delta}{2}\right)\cos\left(\frac{2\pi m}{M}\right) \\ y_{om} = \left(R + \frac{\delta}{2}\right)\sin\left(\frac{2\pi m}{M}\right) \\ x_{im} = \left(R - \frac{\delta}{2}\right)\cos\left(\frac{2\pi m}{M}\right) \\ y_{im} = \left(R - \frac{\delta}{2}\right)\sin\left(\frac{2\pi m}{M}\right) \end{cases}. \tag{22}$$

Then,

$$\mathcal{Q} = q_o\left[\left(R+\frac{\delta}{2}\right)^2 - \left(R-\frac{\delta}{2}\right)^2\right]\sum_{m=1}^{M}\begin{pmatrix} 3\,\cos^2\left(\frac{2\pi m}{M}\right) - 1 & 3\,\cos\left(\frac{2\pi m}{M}\right)\sin\left(\frac{2\pi m}{M}\right) \\ 3\,\cos\left(\frac{2\pi m}{M}\right)\sin\left(\frac{2\pi m}{M}\right) & 3\,\sin^2\left(\frac{2\pi m}{M}\right) - 1\end{pmatrix}. \tag{23}$$

Using that

$$\sum_{m=1}^{M}\begin{pmatrix} 3\cos^2\left(\frac{2\pi m}{M}\right)-1 & 3\cos\left(\frac{2\pi m}{M}\right)\sin\left(\frac{2\pi m}{M}\right) \\ 3\cos\left(\frac{2\pi m}{M}\right)\sin\left(\frac{2\pi m}{M}\right) & 3\sin^2\left(\frac{2\pi m}{M}\right)-1 \end{pmatrix} = \begin{pmatrix} \frac{M}{2} & 0 \\ 0 & \frac{M}{2} \end{pmatrix}, \tag{24}$$

we have

$$\mathcal{Q} = q_o R\delta M\, \mathbb{I}. \tag{25}$$

Using Eq. (19) for q_o, we finally obtain the expression for the quadrupole moment,

$$\mathcal{Q} = eR\delta M\, \mathbb{I}\left[\sum_{\theta_+}\left(\frac{\cos[\theta_+]\sinh[\Delta]}{\sqrt{1+4\cos[\theta_+]^2\sinh[\Delta]^2}}\right) - \sum_{\theta_-}\left(\frac{\cos[\theta_-]\sinh[\Delta]}{\sqrt{1+4\cos[\theta_-]^2\sinh[\Delta]^2}}\right)\right], \tag{26}$$

which can be considered as the main theoretical result of the article. It connects the curvature of the ring with the quadrupole moment.

We first observe that in the continuum limit, when $M \to \infty$, the sums become

$$\left[\sum_{\theta_+}\left(\frac{\cos[\theta_+]\sinh[\Delta]}{\sqrt{1+4\cos[\theta_+]^2\sinh[\Delta]^2}}\right) - \sum_{\theta_-}\left(\frac{\cos[\theta_-]\sinh[\Delta]}{\sqrt{1+4\cos[\theta_-]^2\sinh[\Delta]^2}}\right)\right] \to \frac{M}{2\pi}\left[\int_{\frac{2\pi}{3}}^{\frac{4\pi}{3}}\frac{\cos[\theta]\sinh[\Delta]d\theta}{\sqrt{1+4\cos[\theta]^2\sinh[\Delta]^2}} - \int_{\frac{\pi}{3}}^{\frac{5\pi}{3}}\frac{\cos[\theta]\sinh[\Delta]d\theta}{\sqrt{1+4\cos[\theta]^2\sinh[\Delta]^2}}\right], \tag{27}$$

where we have used $d\theta \to \frac{2\pi}{M}$. Since, in that limit, both integrals are exactly the same, we obtain $\mathcal{Q} = 0$ as expected: no flexoelectric effect for long molecules with small curvature.

Of course, the important question is what range of parameters are physically relevant since that will give an idea of the threshold molecular length below which flexoelectricty becomes relevant. To gain insight into that question, we consider here the case of the recently synthesized cyclo[n]carbons.[21] Although our two-ring structure is not the same as the synthesized cyclo[n]carbons, it can give us an idea of order of magnitude. From Ref. 22 for Carbon, $\delta \cong 1.5$ Å and $\cong 2$ Å^{-1}, so we consider Eq. (26) with $\Delta = \frac{\pi\kappa\delta}{M-1} \cong \frac{3.0\,\pi}{M-1}$ and perform the sums numerically up to the Fermi energy. Figure 3 shows, as a result of that computation, the dependence of $\mathcal{Q}$ on the size of molecule M.

Figure 3 also shows that, for large values of M, we do recover numerically that the quadrupole moment vanishes. But, more interestingly, we see that for up to $M \approx 20$, the quadrupole moment remains larger than 20% of the largest value for $M = 3$.

An interesting value is $M = 9$ since the cyclo[18]-carbon has been synthesized.[21] We see, from Fig. 3, that in this case, the quadrupole value is well above the values corresponding to large molecules (for example, $M = 50$) in Fig. 3.

While our theory focuses on ring molecules, it is worth highlighting the results by Kalinin and Meunier.[6] They performed *ab initio* first principles' density functional theory computations chemistry of carbon structures by NWCHEM.[23] In particular, they considered 20-carbon long polyacetylene chains for different radii of curvature. Because in their study the chains were open, dipole moments were induced. In contrast in our case, by the intrinsic ring nature of the molecules, the dipole moment is zero, and the two results cannot strictly be compared. However, given the similarities of focus between the two approaches, namely, the use of quantum mechanics to elucidate flexoelectricity, it is worth estimating what our theory would provide for open chains. To that end, we first consider a ring 20-atoms long and compute its charge transfer. We use that charge transfer figure to subsequently calculate the dipole moment of 20-atom long open chains of varying radii of curvature. The results are shown in Fig. 4 and are of the same order of magnitude as those obtained by Kalinin and

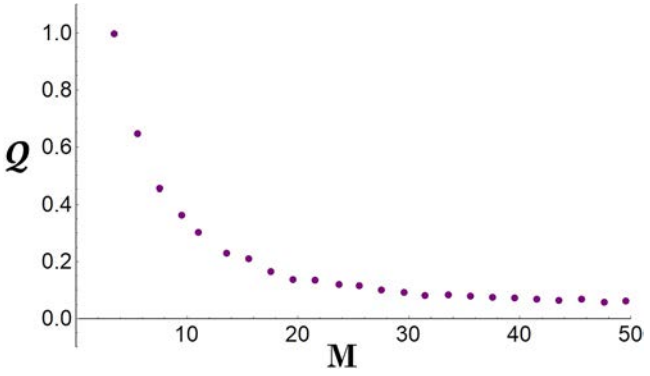

FIG. 3. Induced quadrupole moment $\mathcal{Q}$ vs bending for $\kappa\delta \cong 3$. $\mathcal{Q}$ is given relative to its larger value when $M = 3$.

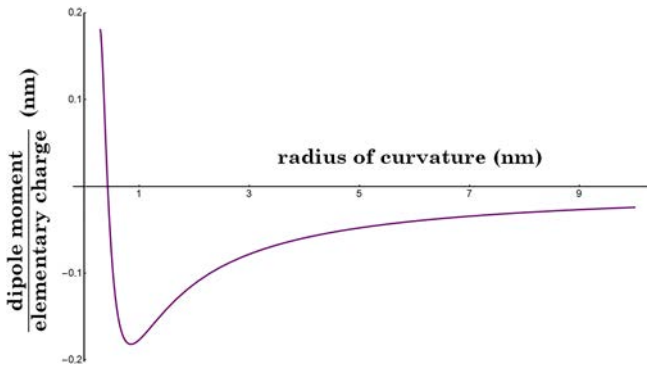

FIG. 4. Dipole moment vs the radius of curvature of a 20-carbon long open double chain.

Meunier. That the results are not the same is, of course, expected since we are doing an estimate and because our double molecule is not the same as polyacetylene. Yet, the closeness of the results is indicative that molecular chains show relevant quantum flexoelectric response in the nanometer range.

V. CONCLUSIONS

While it is known that flexoelectricity is a property of all materials regardless of symmetry or chemical nature, and that its effect increases as the sample size decreases, it is necessary to continue finding unambiguous connections between theory and experiments to be able to assess real systems. This is the more important as the community will grow in its applications of flexoelectricity in nanodevices. It is still a very exciting work in progress.

This article contributes in that direction by establishing a simple criterium to estimate the threshold radius of curvature of bent linear molecules below which flexoelectricity becomes significant. We have given an example of the application of the method to the recently synthesized cyclo[n]carbon ring-shaped organic molecules.

The quantum mechanics framework developed here is easily generalizable to more complicated molecules and to two- and three-dimensional materials. There is no conceptual difficulty, just more time-consuming computations. Here, we restricted to a simple system aiming at understanding the concept rather than doing long computations.

We mentioned in the article already the timeliness of the result, since the measurement of charge at the nanoscale is now becoming quantitatively possible.[15] We complement this comment by the fact that the system presented here is particularly amenable of being probed by atomic force microscopy.[24,25]

ACKNOWLEDGMENTS

Funding for this project comes from the U.S. National Science Foundation under Grant No. CHE-1508085.

DATA AVAILABILITY

The data that support the findings of this study are available from the corresponding author upon reasonable request.

REFERENCES

[1]S. M. Kogan, "Piezoelectric effect during inhomogeneous deformation and acoustic scattering of carriers in crystals, Sov," Phys. Solid State **5**, 2069 (1964).
[2]E. V. Bursian and O. I. Zaikovskii, "Changes in the curvature of a ferroelectric film due to polarization," Sov. Phys. Solid State **10**, 1121 (1968).
[3]A. Abdollahi, N. Domingo, I. Arias, and G. Catalán, "Converse flexoelectricity yields large piezoresponse force microscopy signals in non-piezoelectric materials," Nat. Commun. **10**, 1266 (2019).
[4]J. Hong and D. Vanderbilt, "First-principles theory of frozen-ion flexoelectricity," Phys. Rev. B **84**, 180101(R) (2011).
[5]M. Stengel, "Flexoelectricity from density-functional perturbation theory," Phys. Rev. B **88**, 174106 (2103).
[6]S. V. Kalinin and V. Meunier, "Electronic flexoelectricity in low-dimensional systems," Phys. Rev. B **77**, 033403 (2008).
[7]A. K. Tagantsev, "Piezoelectricity and flexoelectricity in crystalline dielectrics," Phys. Rev. B **34**, 5883 (1986).
[8]J. Hong and D. Vanderbilt, "First-principles theory and calculation of flexoelectricity," Phys. Rev. B **88**, 174107 (2013).
[9]M. Stengel, "Unified *ab initio* formulation of flexoelectricity and strain-gradient elasticity," Phys. Rev. B **93**, 245107 (2016).
[10]P. Zubko, G. Catalán, and A. K. Tagantsev, "Flexoelectric effect in solids," Annu. Rev. Mater. Res. **43**, 387 (2013).
[11]J. Narvaez, F. Vásquez-Sancho, and G. Catalán, "Enhanced flexoelectric-like response in oxide semiconductors," Nature **538**, 219–221 (2016).
[12]J. Narvaez, S. Saremi, J. Hong, M. Stengel, and G. Catalán, "Large flexoelectric anisotropy in paraelectric barium titanate," Phys. Rev. Lett. **115**, 037601 (2015).
[13]A. Abdollahi, F. Vásquez-Sancho, and G. Catalán, "Piezoelectric mimicry of flexoelectricity," Phys. Rev. Lett. **121**, 205502 (2018).
[14]L. Li, S. J. Eppell, and F. R. Zypman, "Method to quantify nanoscale surface charge in liquid with atomic force microscopy," Langmuir **36**, 4123 (2020).
[15]L. Li, N. F. Steinmetz, S. J. Eppell, and F. R. Zypman, "Charge calibration standard for atomic force microscope tips in liquids," Langmuir **36**, 13621 (2020).
[16]N. W. Ashcroft and N. D. Mermin, *Solid State Physics* (Saunders College, Philadelphia, PA, 1976), Chap. 10.
[17]F. R. Zypman and L. F. Fonseca, "Electron-diffraction effects on scanning tunneling spectroscopy," Phys. Rev. B **55**, 15012 (1997).
[18]P. W. Atkins, *Molecular Quantum Mechanics*, 2nd ed. (Oxford University Press, Oxford, NY, 1993), p. 254.
[19]J. D. Jackson, *Classical Electrodynamics*, 2nd ed. (Wiley, New York, 1975), Chap. 4.
[20]I. V. Lindell, *Methods for Electromagnetic Field Analysis* (Wiley-Blackwell, New York, 1996), Chap. 2.
[21]K. Kaiser, L. M. Scriven, F. Schulz, P. Gawel, L. Gross1, and H. L. Anderson, "An sp-hybridized molecular carbon allotrope, cyclo[18]carbon," Science **365**, 1299–1301 (2019).
[22]D. Papaconstantopoulos, M. Mehl, S. Erwin, and M. Pederson, "Tight-binding Hamiltonians for carbon and silicon," MRS Online Proc. Libr. **491**, 221 (1997),
[23]M. Valiev, E. J. Bylaska, N. Govind, K. Kowalski, T. P. Straatsma, H. J. J. van Dam, D. Wang, J. Nieplocha, E. Apra, T. L. Windus, and W. A. de Jong, "NWChem: A comprehensive and scalable open-source solution for large scale molecular simulations," Comput. Phys. Commun. **181**, 1477 (2010).
[24]D. Lazarev and F. R. Zypman, "Charge and size of a ring in an electrolyte with atomic force microscopy," J. Electrost. **87**, 243 (2017).
[25]D. Lazarev and F. R. Zypman, "Determination of charge and size of rings by atomic force microscopy," J. Electrost. **83**, 69 (2016).